IOP Publishing Superconductor Science and Technology
Supercond. Sci. Technol. 30 (2017) 074006 (9pp) https://doi.org/10.1088/1361-6668/aa6fbe

Fourcross shaped metamaterial filters fabricated from high temperature superconducting YBCO and Au thin films for terahertz waves

Y Demirhan[1], H Alaboz[1], M A Nebioğlu[2], B Mulla[1], M Akkaya[2], H Altan[2], C Sabah[3] and L Ozyuzer[1]

[1] Department of Physics, Izmir Institute of Technology, Urla, 35430, Izmir, Turkey
[2] Department of Physics, Middle East Technical University, Çankaya, 06800, Ankara, Turkey
[3] Department of Electrical and Electronics Engineering, Middle East Technical University—Northern Cyprus Campus, Kalkanli, Güzelyurt, TRNC/Mersin, Turkey †

E-mail: ozyuzer@iyte.edu.tr

Received 27 December 2016, revised 21 April 2017
Accepted for publication 27 April 2017
Published 9 June 2017

Abstract

In this study, we present a new, unique fourcross shaped metamaterial terahertz (THz) filter fabricated from both gold thin films and $YBa_2Cu_3O_{7-d}$ high T_c superconducting thin films. A commercial electromagnetic simulation software, CST Microwave Studio, is used to design and optimize the metamaterial filter structures. The proposed fourcross shaped rectangular filter structure consists of periodic metallic rings where strip lines are located at the sides of the ring. Fourcross metamaterial filters are fabricated by using e-beam lithography and ion beam etching techniques. Terahertz time-domain spectroscopy measurements validated the design predictions for both the center frequencies and bandwidths of the resonances due to the fourcross structures. The resonance switching of the transmission spectra was investigated by lowering the temperature below the critical transition temperature. This resonance switching effect is not observed in filters made up of metals. This novel fourcross rectangular resonator with a temperature-dependent resonance behavior holds great potential for active, tunable and low loss THz devices for imaging, sensing, and detection applications.

Keywords: metamaterial, superconductor, terahertz, time domain spectroscopy, YBCO

(Some figures may appear in colour only in the online journal)

1. Introduction

Terahertz (THz) radiation is a part of the electromagnetic spectrum lying between microwaves and the infrared. This region covers frequencies ranging from 0.3 to 10 THz and wavelengths from 1 to 0.03 mm. Organizations involved in military and defense are requesting the development of many technologies such as hand held THz radar systems that work in this frequency range to remotely detect the presence of explosive materials, poison gases, ceramic weapons, and biological warfare agents like viruses and bacteria [1–6]. In addition, the medical community has shown that THz waves can detect the presence of cancer, viruses, bacteria, and other diseases instantly without surgery, biopsies, or other expensive procedures making this an ever more important area for further research and development [7]. These coupled with a large variety of possible applications from pharmaceuticals to agricultural research is feeding the demand to develop compact and tunable coherent THz devices. The frequency range between 0.1 and 10 THz is usually called the THz gap as it is difficult to develop devices

† Publisher's note: Whilst IOP Publishing adheres to and respects UN resolutions regarding the designations of territories (available at http://www.un.org/press/en), the policy of IOP Publishing is to use the affiliations provided by its authors on its published articles.

 © 2017 IOP Publishing Ltd Printed in the UK

which can interact, generate or detect radiation since bulk materials typically do not exhibit a strong electromagnetic response in this region. There are notable attempts aiming to fill this vacancy in the spectrum [8–12].

For THz applications, metamaterials which can be designed with a specific functionality have a crucial role in the fabrication of artificial optical components since they have electromagnetic properties which could not be achieved by their natural bulk material counterparts. In its most basic form, the metamaterial structure can be thought of as electrical circuits much less in size than the wavelength that replace atoms as the basic unit of interaction with electromagnetic radiation. This field has seen a notable progress in recent years [13, 14] where studies have led to the development of electromagnetic metamaterials which exhibit novel properties such as magnetic response at terahertz and optical frequencies, negative index of refraction, and huge chirality [15, 16]. The emergence of THz metamaterials has given rise to electromagnetic properties and functionality that can not be attained by already existing natural materials permitting a whole new family of metamaterial based devices namely, electrically small resonators, compact high selective THz filters, superlenses, cloaks, chiral devices, electromagnetically induced transparency applications and modulators. Consequently, the theoretical and experimental study of THz metamaterials has attracted great attention [17–19]. Conventional THz metamaterials are typically fabricated from either dielectrics or normal conducting metals. While sub-wavelength structures based on these conventional materials have shown low insertion loss at microwave frequencies, substantial losses exhibited in the terahertz frequency range have been one of the key limitations, and this remains a driving force to explore novel structures based on novel materials to minimize losses. Other factors which can effect the performance include the conductivity of the metamaterial which imposes a severe limit on the device performance in the THz frequency range (the degree of Ohmic loss can be measured by the quality factor Q of the resonance) [20].

In contrast to normal conducting metals, electromagnetic properties possessed by superconductors can be utilized for the purpose of producing almost ideal and novel metamaterial structures. If metallic structures are replaced by superconducting structures losses can be greatly reduced [21]. The complex conductivity of superconductors intrinsically depends on the applied magnetic field and temperature in comparison to metals. This allows the possibility to directly control the conductivity of the superconducting element without inserting additional elements i.e. an active metamaterial structure [22, 23]. Moreover, superconductors show superior conductivity at low temperatures and have the potential to integrate elements exhibiting quantum behavior. In these materials, values of the surface resistance at microwave frequencies are also small [24].

The unique properties of superconducting materials allow them to be utilized in a number of ways for THz device applications. Momentarily, Josephson based metamaterials propose a lot of important and attractive opportunities for novel metamaterial structures. The nonlinear response of these materials can allow for parametric amplification [25] of photons and also reduction of losses. Moreover, in accordance with the changes in the Josephson inductance, superconducting meta-atoms can display an intrinsic tunability of their resonance frequency by magnetic field and temperature. The suppression of the superconducting order parameter, i.e. the density of Cooper pairs leads to the tunability. In superconductor metamaterials, the quality factor of the resonance can also be altered by tuning the resonance frequency. Measurement of a field-induced nonlinear response of metamaterials and unpatterned films made out of the low-T_c conventional superconductor NbN has been reported by Zhang *et al* [26]. Here, the gap frequency (f_g) of NbN is given by $f_g = 2\Delta_0/h$, where Δ_0 is the energy gap at 0 K and h is the Planck constant at 1.18 THz [27]. In contrast, high-T_c superconductors are more appropriate for a broadband response since they have a larger energy gap. High-T_c cuprate superconducting materials exhibit metallic behavior for currents flowing in the Cu–O planes, and possess dielectric-like properties for light polarized in the c-direction. Moreover, they have higher transition temperatures, which ensure conduction of electrical current without resistance at liquid nitrogen temperatures—the requirement to create and maintain a cryogenic environment being the main disadvantage of superconductors.

Measurement of the nonlinear THz transmission through films composed of the high-T_c superconductor $YBa_2Cu_3O_7$ (YBCO) has been performed by Glossner *et al* [28]. In a similar fashion Orenstein *et al* [29] measured the nonlinear transmission of BSSCO at modest field strengths finding a characteristic current scale for the nonlinearity on the order of the intrinsic depairing current for $Bi_2Sr_2CaCuO_{8+x}$ (BSSCO) that can be calculated from well-known parameters. Latter works concentrated in minimizing the material losses, by cautiously designing metamaterial structures to match impedances between propagation in different media. Wire structures are useful in tuning the negative permittivity while structures such as split-ring resonators have been shown to be useful where temperature dependent tuning of the negative permeability in the superconducting structure can be implemented [16, 30].

In this study, the aim was to design superconducting metamaterial filters with a unique geometry which operates in the THz frequency band. Both normal conductive metallic films and high T_c superconductor YBCO thin films were employed in the patterning of the structures. By modifying the geometrical parameters of the structure and temperature dependent superconducting properties it is shown that both the resonance frequency and transmittance at resonance of the metamaterial structure can be tuned. These properties provide the means to fabricate very efficient and compact metamaterial-based filters with a high selectivity. These type of highly particular filters can be used to delete undesirable transmitted signals in pre-defined frequency bands and have potential applications in the field of THz diagnostics.

2. Design and fabrication of fourcross metamaterial filters

2.1. Design and background theory

A unique geometry that can be used as a terahertz filter which operates in the sub THz frequency range has been designed. In

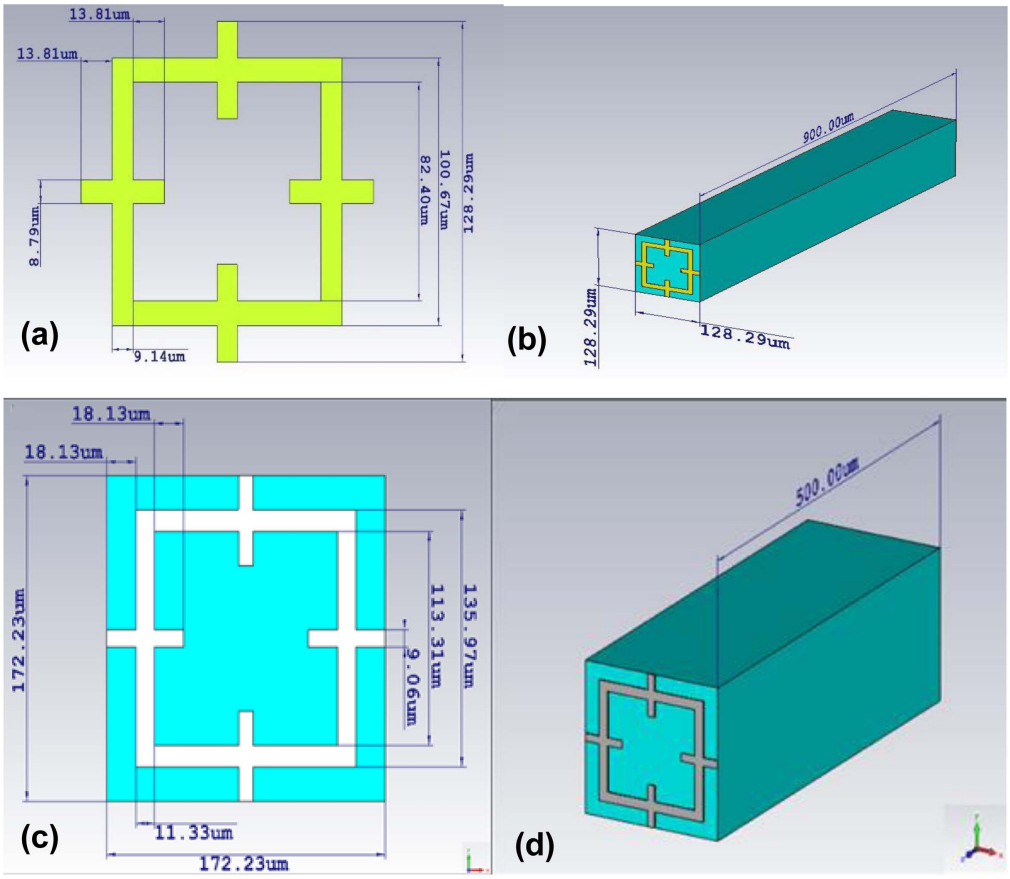

Figure 1. (a), (b) Front and perspective view of gold fourcross filter design with the unit cell dimensions; the width of the unit cell (W) was 128.29 μm, the length of the square-loop (L) was 100.67 μm, and the width of the strip line (M) was 8.79 μm. (c), (d) Front and perspective view of YBCO fourcross filter design with the unit cell dimensions; the width of the unit cell (W) was 172.23 μm, the length of the square-loop (L) was 135.97, and the width of the strip line (M) was 9.06 μm.

figure 1, the design of the filter structure is presented in detail. The structure of the metamaterial, namely a fourcross rectangular resonator, has a rectangular shape where strip lines are located at the sides of the ring on a dielectric substrate (figures 1(a), (c)).

The proposed design has not split rings or evident capacitance elements. This is the combination of square ring with quadruple strips. In general, for metamaterial structures, LC equivalent circuit model can be used to predict the resonance behavior of the metamaterial design. The simplified form of the equivalent circuit of the proposed design is given in figure 2(a). For the given structure, the inner gap between the strips behaves as capacitor where the metallic parts behave as inductors. In addition, C represents the capacitance formed by the gap between the mutual strips.

The total capacitance can be calculated by the parallel plate capacitance formula [31]:

$$C_1 = KW\varepsilon_0 \frac{2}{\pi} \ln \frac{H}{S}, \tag{1}$$

$$C_2 = KW\varepsilon_0 \frac{\varepsilon_s - 1}{\frac{s}{h_s}}, \tag{2}$$

$$C = C_1 + C_2. \tag{3}$$

Here $K = n\frac{\omega}{c}$, ε_o is the free space permittivity, ε_s represents the dielectric constant of the substrate h_s is the thickness of the substrate. The values and the placement of the symbols used in the equations (1)–(3) (H, W, S) is given in the figure 2(b). Total inductance can be calculated by using the formula [32],

$$L = \frac{\mu_0 l}{2\pi}\left[\ln\left(\frac{2l}{b}\right) + \frac{l}{2} + \frac{b}{3l} - \frac{b^2}{24l^2}\right], \tag{4}$$

where the length and the width of the metallic strips are given by the symbols l and b respectively.

From the equations (1)–(4) the values for K, C_1, C_2 and L are obtained as follows

$$K = 105.19,$$

$$C_1 = 1.94 \times 10^{-15}\,\text{F},$$

$$C_2 = 1.59 \times 10^{-18}\,\text{F},$$

$$L = 1.6 \times 10^{-11}\,\text{H}.$$

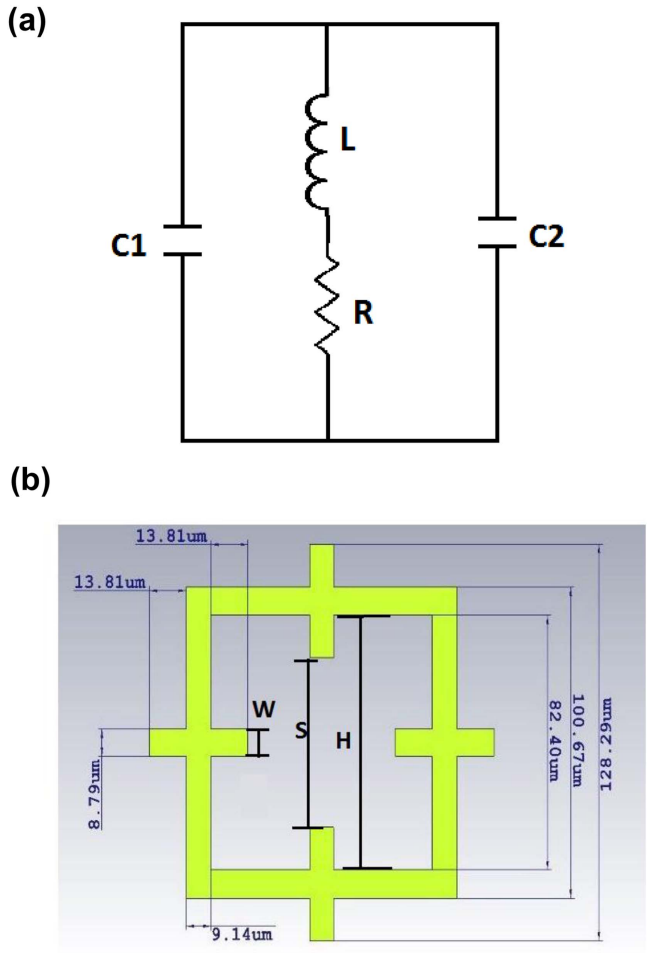

Figure 2. (a) Equivalent circuit of the proposed design. (b) The placement of the symbols used in the equations (1)–(3), (*H*, *W*, *S*).

The resonance frequency depends on the total capacitance and the total inductance of the circuit and it can be calculated using the relation:

$$f_0 = \frac{1}{2\pi}\sqrt{\frac{1}{L(C1+C2)}}. \quad (5)$$

The resonance frequency obtained from the calculations is $f_0 = 0.90$ THz which is very close to the experimental resonance at 0.92 THz.

The fourcross resonator is designed in accordance with the fact that the observed resonance takes place in the low frequency THz range which is approachable with the small energy gap observed in high-T_c superconducting materials. In order to investigate the transmission profile and provide an optimal design, CST Microwave Studio software frequency domain solvers are used. After these steps the devices are patterned on the selected dielectric substrates and measurements are performed using THz time domain spectroscopy (THz-TDS) technique.

Initially the simulations are carried out using 130 nm thick patterned gold layer and 80 nm thick patterned YBCO layer deposited on 900 μm thick fused silica and 500 μm thick sapphire substrates respectively. These substrates are commonly used to fabricate filter structures since they show negligible loss

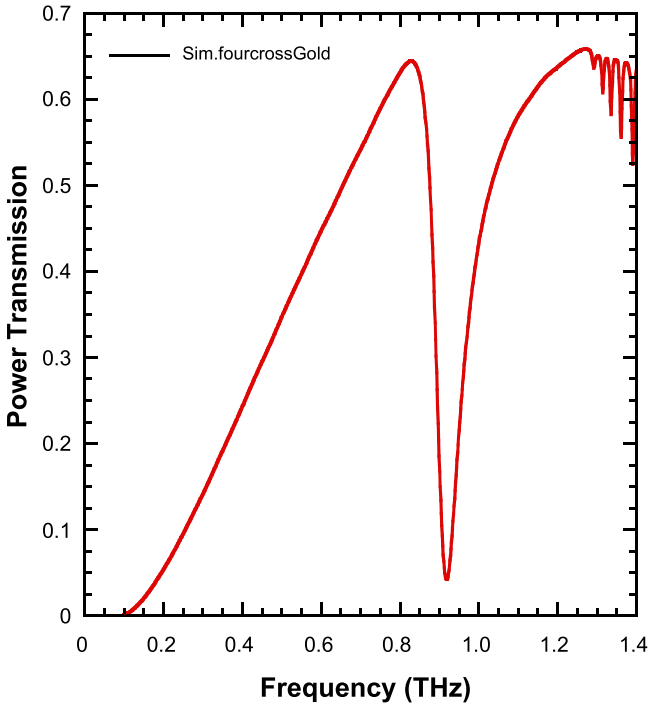

Figure 3. The simulated transmission spectrum of gold fourcross filters with designed parameters (solid line).

at THz frequencies. For the simulations, the electrical permittivity values are extracted by THz-TDS measurements of the fused silica and sapphire substrates in the THz region. Electrical permittivity and loss tangent for fused silica are $\varepsilon_r = 3.98$, $\tan\delta = 0.05$ whereas for sapphire they are $\varepsilon_r = 9.6$, $\tan\delta = 0.05$. Gold fourcross filters have been designed with the following mesh parameters; the width of the unit cell (W) was 128.29 μm, the length of the square-loop (L) was 100.67 μm, and the width of the strip line (M) was 8.79 μm as shown in figures 1(a) and (c). The numerical results for terahertz wave transmittance of the gold metamaterial filter on 900 μm fused silica are shown in figure 3, where the initial simulated results for the band-stop filter design give the terahertz wave minimum transmittance peak at 0.92 THz. In contrast to gold fourcross filters, YBCO fourcross filters can be tuned by varying the temperature. To investigate the temperature-dependent resonance behavior and confirm the measurements, simulations are carried out at temperatures above and well below T_c.

The tunable characteristics of THz transmission principally originates from the temperature-dependent conductivity in the superconductor material. Using the two-fluid model, the change in the density of superconducting and normal carriers leads to the change in the conductivity of the material [33]. An increase in the temperature of the superconductor decreases the density of superconducting Cooper pairs with respect to the normal conduction electron population which takes place up to state where the Cooper pair density goes to zero at T_c governing the conductivity of the superconductor.

For YBCO, under the two-fluid model, the normal state carriers whose motion obeys the Drude model contributes to the real part of the conductivity σ_r, on the other hand the imaginary part σ_i is determined by the superconducting

carriers, which obeys the London equation hereby the conductivity of the superconducting carriers can be described as $\sigma_i = i(n_s e^2)/(m^*\omega)$ where n_s is the Cooper pair carrier density, e is the charge of carriers, m^* is the effective carrier mass, and ω is the frequency of operation [34]. It is important to emphasize that the conductivity resulting from the Cooper pairs is purely imaginary and consequently the resistivity of the YBCO below T_c is also almost imaginary, and this fact gives rise to an inductor type behavior under the applied THz field. As it is well known; the absolute value of the imaginary conductivity is three orders of magnitude less than the real part, in the THz regime, and thus at temperatures higher than T_c the real part of conductivity is superior [35]. Furthermore, several K under T_c, the imaginary conductivity value increases rapidly with decreasing temperatures and then the total conductivity is dominated by σ_i.

Using this model the complex conductivity of the superconductor material for different temperatures is calculated as a function of frequency using the equations given below. Using calculated conductivity values and thickness of the metamaterial, the surface impedance of the superconducting thin film is obtained and fed into the simulation program to simulate the transmission of the THz waves through the fourcross YBCO filters [36].

Appropriate with the two-fluid model [33], the real and imaginary parts of the conductivity are given by,

$$\sigma_{re} = \frac{ne^2}{m^*}\frac{f_n(T)\tau}{1+\omega^2\tau^2} = \frac{ne^2\varepsilon_0}{m^*\varepsilon_0}\frac{f_n(T)\tau}{1+\omega^2\tau^2} = \omega_p^2\varepsilon_0\frac{f_n(T)\tau}{1+\omega^2\tau^2}, \tag{6}$$

$$\begin{aligned}\sigma_{im} &= \frac{ne^2}{m^*}\left[\frac{f_n(T)\omega\tau^2}{1+\omega^2\tau^2}\frac{f_s(T)}{\omega}\right] \\ &= \frac{ne^2\varepsilon_0}{m^*\varepsilon_0}\left[\frac{f_n(T)\omega\tau^2}{1+\omega^2\tau^2}\frac{f_s(T)}{\omega}\right] \\ &= \omega_p^2\varepsilon_0\left[\frac{f_n(T)\omega\tau^2}{1+\omega^2\tau^2}\frac{f_s(T)}{\omega}\right],\end{aligned} \tag{7}$$

where n is the carrier density, m^* is the carrier effective mass, and τ is the quasiparticle relaxation time. The ratio of normal to superconducting carriers is,

$$f_n(T) + f_s(T) = 1, \tag{8}$$

where f_n and f_s are fractions of normal (quasiparticle) and superconducting (superfluid) carriers. The inverse relaxation time is given by,

$$\frac{1}{\tau(t)} = \frac{1}{\tau(1)}\frac{t}{1+\alpha(t^{1-\gamma}-t)}, \tag{9}$$

where t is the ratio of the temperatures and is defined as,

$$t = \frac{T}{T_c} \tag{10}$$

and α is an exponent in addition γ is an empirical parameter. Using these relations the conductivity and surface impedance of the patterned films are,

$$\sigma = \sigma_{re} + i\sigma_{im}, \tag{11}$$

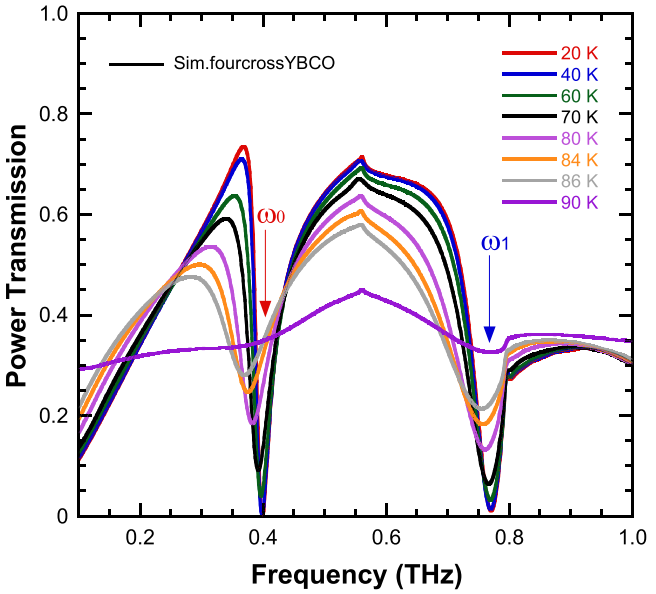

Figure 4. The simulated transmission spectrum of YBCO fourcross filters with designed parameters.

$$Z_s = R_s + iX_s = \sqrt{\frac{i\omega\mu_0}{\sigma}}\coth\left(d\sqrt{i\omega\mu_0\sigma}\right). \tag{12}$$

Optimized design parameters of YBCO fourcross filters are as follows; the width of the unit cell (W) was 172.23 μm, the length of the square-loop (L) was 135.97 μm, and the width of the strip line (M) was 9.06 μm. The results of the YBCO fourcross simulations are presented in figure 4. According to the simulations, the resonances reduced to zero transmission both at the temperatures 20 and 40 K. With the specified mesh dimensions, the simulated YBCO fourcross filter design establishes a stop band at both ω_0 (0.412 THz) and ω_1 (0.765 THz) for 20 K. These resonances shifted to ω_0 (0.410 THz) and ω_1 (0.760 THz) at 40 K, respectively. Furthermore, a resonance shift to ω_0 (0.390 THz) and ω_1 (0.734 THz) at 60 K is also observed.

2.2. Fabrication and measurements

A gold metal film with a thickness of 230 nm is deposited by dc magnetron sputtering system under optimal conditions for the gold metamaterial samples. A commercially available 80 nm thick YBCO film grown on sapphire substrates is used for the superconducting samples (YBCO film is deposited by Ceraco Ceramic Coating GmbH). The transition temperature of the YBCO films, oriented with the *ab* plane parallel to the surface, was measured to be $T_c \cong 90$ K by closed cycle He cryostat system. Conventional e-beam lithography, and ion beam etching techniques were used for the microfabrication of the metamaterial filters.

E-beam lithography is a more precise technique than conventional optical lithography. In UV lithography process, different imperfections could appear as irregularity in shape rounding etc. And it has been shown that these variations in the structure will affect the spectral properties of the THz filters [35]. Figure 5 shows the optical photographs of the cross-shaped

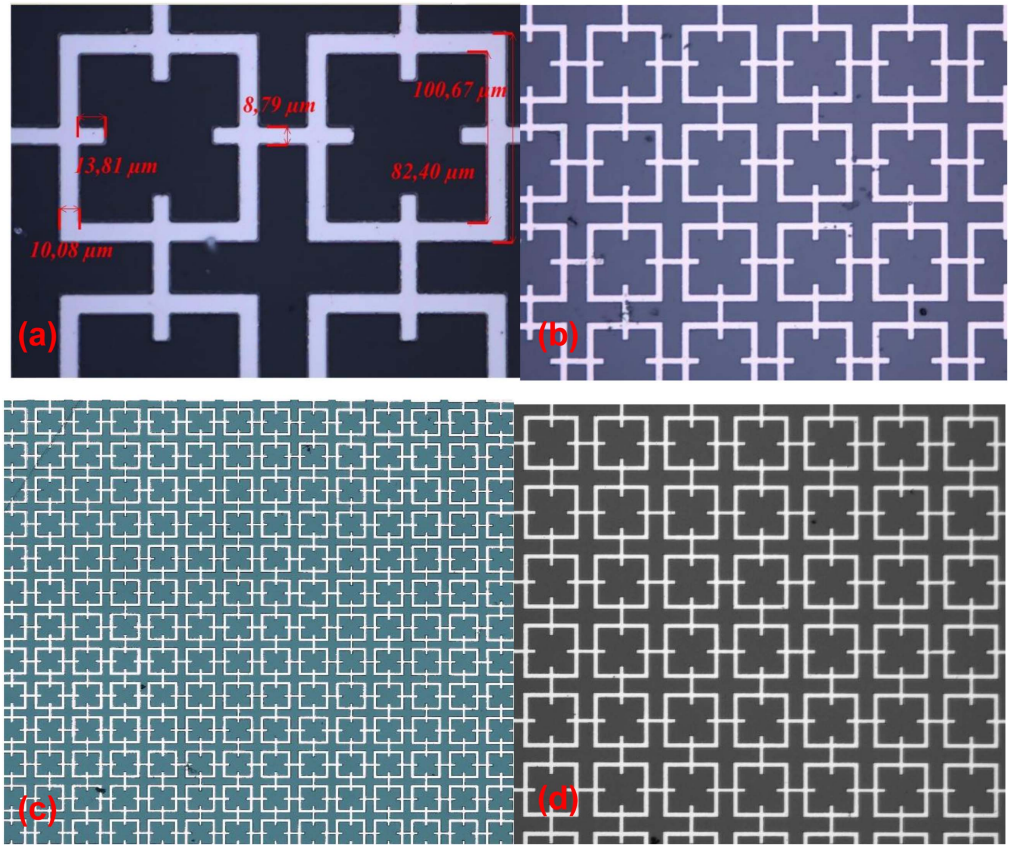

Figure 5. (a) Optical microscope images of fabricated gold fourcross filters given with measured dimensions. (b)–(d) Optical microscope images of fabricated gold and YBCO fourcross filters which is taken with different magnifications.

filters fabricated from both Au and YBCO thin films and we obtain almost perfect structures.

The transmission profile of the fourcross filters were analyzed by a home built THz-TDS system which is driven by a Ti: Al_2O_3 mode-lock laser. The incoming beam is separated by a beam splitter into the generation arm and detection arm of the spectrometer. In the first arm namely, the generation arm, by making use of a multi-dipole photoconductive antenna a s-polarized terahertz beam is produced. With the help of two off-axis parabolic mirrors and two TPX™ polymethylpentene lenses, produced THz rays are guided within the system inside the antenna. In the detection arm, electro-optic detection method through a balanced photodiode is introduced for the measurement of THz pulse. A lock-in amplifier is provided for the utilization of phase-sensitive detection and by making use of a PC and data acquisition software, data is recorded. The frequency data is obtained with 40 GHz resolution after applying a Fourier transform to the time-domain data. Superconducting patterned sample characterization was done with a closed cycle helium cryostat that was installed inside the terahertz time domain spectroscopy system. The cooling system is composed of Sumitomo CH-204SFF coldhead, Sumitomo HC-4A compressor and Vacuubrand RZ 14 vacuum pump. Samples were mounted onto sample holder at the end of the cold head. Via two high quality

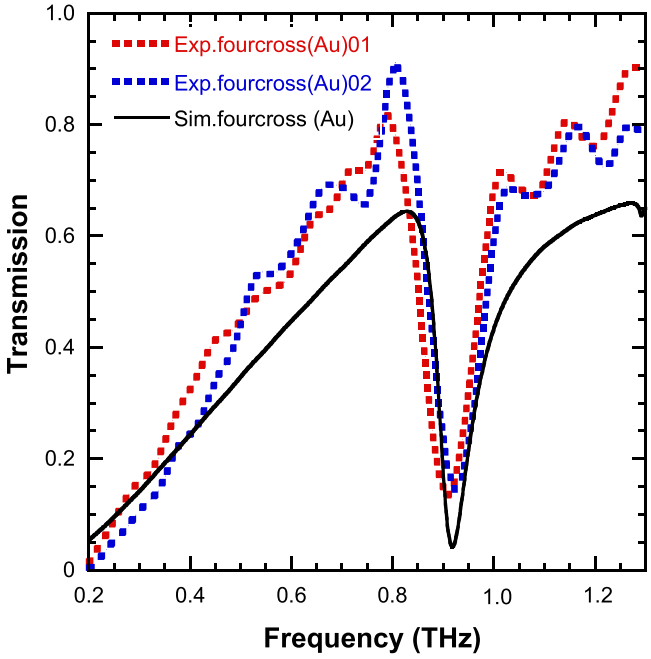

Figure 6. THz time-domain measurements of two identical gold fourcross filters (Fourcross(Au)01-dashed red line- and Fourcross (Au)02-dashed blue line), plotted with simulation results(solid black line) on the same graph.

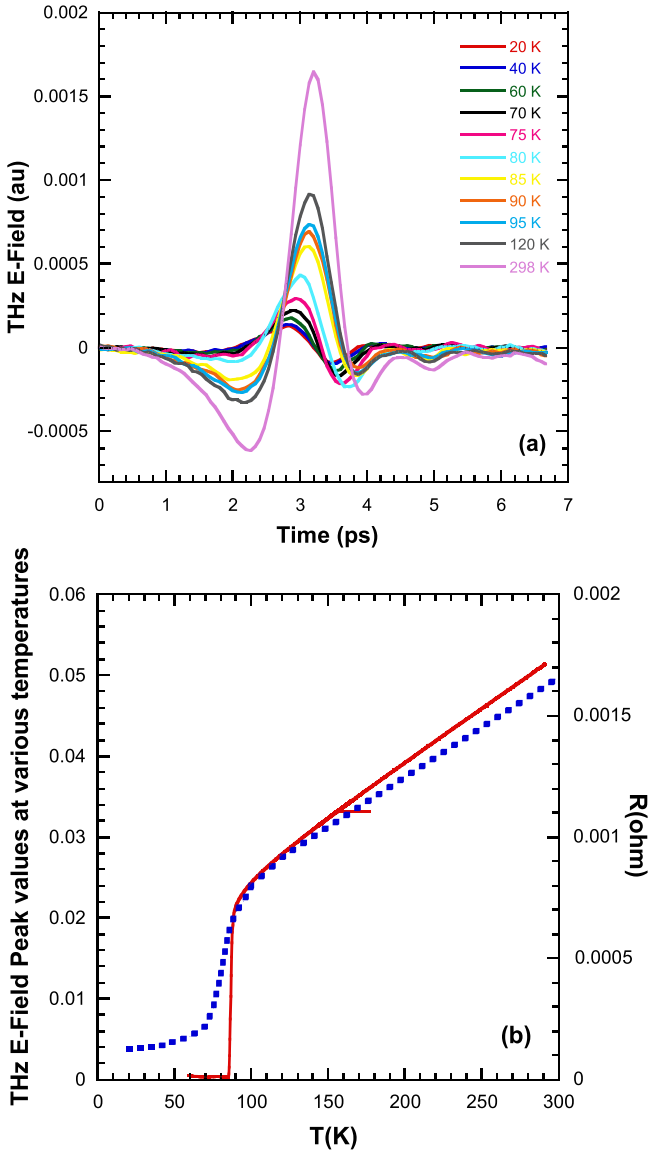

Figure 7. (a) The THz transmission of unpatterned 80 nm thick YBCO film at 20, 40, 60, 65, 70, 75, 80, 85, 90, 95, 100, 120 and 298 K. (b) The THz *E*-field peak values versus temperature curve is plotted in order to determine the critical temperature of the superconducting YBCO film (blue curve). *R*–*T* measurement of the film is also plotted on the same graph (red curve).

quartz windows the THz radiation is focused through the samples.

3. Results and discussion

Figure 6 present the measured transmission spectra for two different gold fourcross samples given together with the simulation results on the same graph (Fourcross(Au)01 and Fourcross(Au)02). The measured electromagnetic properties of the metamaterials are consistent with that of the simulation results. Resonance frequency of this structure is at 0.92 THz according to the simulation results. As seen from figure, sample 1 has a resonance at 0.9 THz, sample 2 has a resonance at 0.92 THz according to THz TDS measurement. As

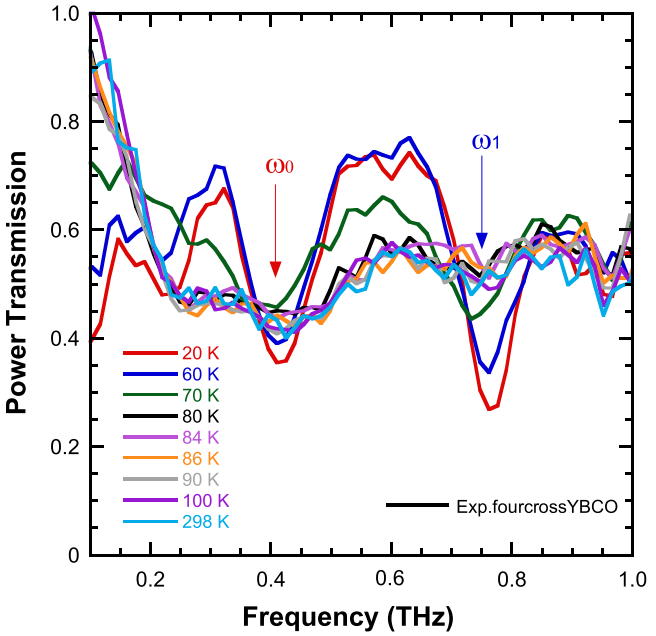

Figure 8. THz time-domain measurement of YBCO fourcross filter taken from 298 to 20 K.

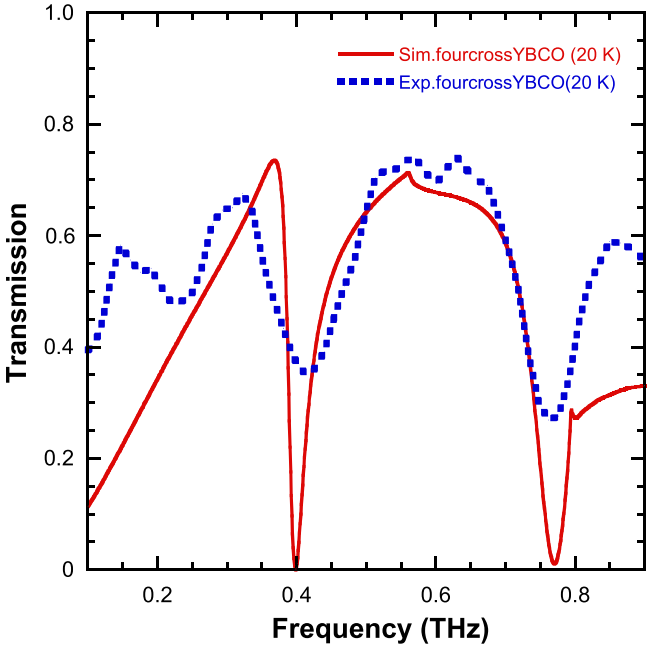

Figure 9. THz time-domain measurement of YBCO fourcross filter at 20 K, plotted with simulation result on the same graph.

expected from numerical analysis, the metamaterial structure consisting of rectangular resonator exhibits bandstop characteristics.

The terahertz transmission of unpatterned single layer 80 nm thick YBCO film at 20, 40, 60, 65, 70, 75, 80, 85, 90, 95, 100, 120 and 298 K is shown in figure 7(a). Below the critical temperature YBCO layer presents metallic characteristics and the transmitted signal power is very low. The THz E-field peak values versus temperature is plotted in order to determine the critical temperature of the superconducting

YBCO film. The graph in figure 7(b) is similar to a superconducting phase transition curve obtained by the *R–T* measurement of the film which is also plotted on the same graph. These show that the critical temperature of the sample is approximately 90 K.

The THz transmission amplitude spectra for the fabricated YBCO metamaterial filter structure at various temperatures are presented in figure 8. In the metamaterial transmission spectra given by the graph, two resonance peaks are observed at ω_0 (0.4 THz) and ω_1 (0.75 THz). The patterned structure exhibits powerful resonances observed at temperatures below T_c, namely, 20 K which is implied by the sharp THz transmission dip ω_1 with a minimal transmission amplitude of 0.05 at ω_0 (0.61 THz). In the figure it is seen that; with a decrease in temperature one observes increase in resonance strength and also a resonance shift to higher frequencies. With the increase of temperature (from 20 K up to T_c and the room temperature) resonance frequency is blue-shifted and it is observed that the resonance strength decreases as a broadening and reduction in amplitude of the transmission dip. THz transmission measurement and simulation result of YBCO fourcross filter at 20 K, which is much lower than T_c, is shown in figure 9 on the same graph. The metamaterial filter exhibits a strong resonance ω_1 at 20 K when compared to other temperatures. A redshift of the resonance frequency ω_1 (7%) is observed as the temperature increases and approaches T_c. The THz transmission amplitude of the band stop filters changes from 26% at 20 K to 53% at 90 K, exhibiting about a 51% change in the amplitude for the ω_1.

For normal conducting metal films, with respect to the temperature changes, the resonance strength and frequency have very small tunability in comparison with the YBCO metamaterials. In a previous study, it is shown that the metamaterials fabricated from thinner YBCO superconducting films will have a lower resonance frequency and will be more efficient in resonance switching and frequency tuning [36].

4. Conclusion

A unique metamaterial based on a fourcross patterned above metallic gold films and thin high temperature superconducting YBCO films has shown that it can be used as an active band-stop filter in the THz frequency region. Resonance switching and frequency shifting are observed in YBCO fourcross filters as a function of the temperature. Simulated results and THz-TDS measurements exhibit that a significant spectral tunability of the resonance can be achieved using YBCO fourcross filters under the critical temperature. These investigations clearly prove the possibility of temperature switched, low loss, THz active devices based on YBCO metamaterials. The THz metamaterial filters fabricated from the high temperature superconductors, integrated with low cost cooling technology, can be used to build and develop THz sources and detectors.

Acknowledgments

This work has been supported in part by TUBITAK (Scientific and Technological Research Council of Turkey) under project number 114F091 and METU research office funded grant BAP-08-011-2016-053. The infrastructure of Applied Quantum Research Center (UKAM) was used to perform some parts of the experiments. Hakan Altan also acknowledges support from BAGEP Award of the Science Academy in Turkey and also the support of the Turkish Academy of Sciences in the framework of the Young Scientist Award Program (TUBA-GEBIP).

References

[1] Tonouchi M 2007 Cutting-edge terahertz technology *Nat. Photon.* **1** 97–105
[2] Kawayama I, Zhang C, Wang H and Tonouchi M 2013 Study on terahertz emission and optical/terahertz pulse responses with superconductors *Supercond. Sci. Technol.* **26** 093002
[3] Ferguson B and Zhang X-C 2006 Materials for terahertz science and technology *Nat. Mater.* **1** 26–33
[4] Kleine-Ostmann T and Nagatsuma T 2011 A review on terahertz communications research *J. Infrared Millim. Terahertz Waves* **32** 143–71
[5] Pickwell E and Wallace V P 2006 Biomedical applications of terahertz technology *J. Phys. D: Appl. Phys.* **39** R301–10
[6] Ozyuzer L *et al* 2007 Emission of coherent THz radiation from superconductors *Science* **318** 1291
[7] Woodward R M, Cole B E, Wallace V P, Pye R J, Arnone D, Linfield E H and Pepper M 2002 Terahertz pulse imaging in reflection geometry of human skin cancer and skin tissue *Phys. Med. Biol.* **47** 3853–63
[8] Kleiner R, Steinmeyer F, Kunkel G and Müller P 1992 Intrinsic Josephson effects in $Bi_2Sr_2CaCu_2O_8$ single crystals *Phys. Rev. Lett.* **68** 2394
[9] Kadowaki K *et al* 2008 Direct observation of terahertz electromagnetic waves emitted from intrinsic Josephson junctions in single crystalline $Bi_2Sr_2CaCu_2O_{8+\delta}$ *Physica* C **468** 634–9
[10] Wang H B, Guénon S, Yuan J, Iishi A, Arisawa S, Hatano T, Yamashita T, Koelle D and Kleiner R 2009 Hot spots and waves in $Bi_2Sr_2CaCu_2O_8$ Intrinsic Josephson junction stacks-a study by low temperature scanning laser microscopy *Phys. Rev. Lett.* **102** 017006
[11] Guénon S *et al* 2010 Interaction of hot spots and THz waves in $Bi_2Sr_2CaCu_2O_8$ intrinsic Josephson junction stacks of various geometry *Phys. Rev.* B **82** 214506
[12] Demirhan Y, Saglam H, Turkoglu F, Alaboz H, Ozyuzer L, Miyakawa N and Kadowaki K 2015 Area dependence and influence of crystal inhomogeneity on superconducting properties of Bi2212 mesa structures *Vacuum* **120** 89–94
[13] Smith D R, Pendry J B and Wiltshire M C K 2004 Metamaterials and negative refractive index *Science* **305** 788
[14] Soukoulis C M and Wegener M 2010 Materials science. Optical metamaterials–more bulky and less lossy *Science* **330** 1633
[15] Hsieh F J, Wang W C and Chang C L 2012 Full extraction methods to retrieve effective refractive index and parameters of a bianisotropic metamaterial based on material dispersion models *J. Appl. Phys.* **112** 064907
[16] Padilla W J, Taylor A J, Highstrete C, Lee M and Averitt R D 2006 Dynamical electric and magnetic metamaterial response at terahertz frequencies *Phys. Rev. Lett.* **96** 107401

[17] Chen H T, O'Hara J F, Azad A K, Taylor A J, Averitt R D, Shrekenhamer D and Padilla W J 2008 Experimental demonstration of frequency-agile terahertz metamaterials *Nat. Photon.* **2** 295–8
[18] Chen H T, Padilla W J, Zide J M O, Gossard A C, Taylor A J and Averitt R D 2006 Active terahertz metamaterial devices *Nature* **444** 597–600
[19] Linden S, Enkrich C, Wegener M, Zhou J, Koschny T and Soukoulis C M 2004 Magnetic response of metamaterials at 100 terahertz *Science* **306** 1351–3
[20] Singh R, Tian Z, Han J, Rockstuhl C, Gu J and Zhang W 2010 Cryogenic temperatures as a path toward high-Q terahertz metamaterials *Appl. Phys. Lett.* **96** 071114
[21] Ricci M C, Xu H, Prozorov R, Zhuravel A P, Ustinov A V and Anlage S M 2007 Tunability of superconducting metamaterials *IEEE Trans. Appl. Supercond.* **17** 918–21
[22] Zhang C H, Wu J B, Jin B B, Ji Z M, Kang L, Xu W W, Chen J, Tonouchi M and Wu P H 2012 Low-loss terahertz metamaterial from superconducting niobium nitride films *Opt. Express* **20** 42–7
[23] Chen H-T, Yang H, Singh R, O'Hara J F, Azad A K, Trugman S A, Jia Q X and Taylor A J 2010 Tuning the resonance in high-temperature superconducting terahertz metamaterials *Phys. Rev. Lett.* **105** 247402
[24] Savinov V, Fedotov V A, Anlage S M, Groot P A J D and Zheludev N I 2012 Modulating sub-THz radiation with current in superconducting metamaterial *Phys. Rev. Lett.* **109** 243904
[25] Kurter C, Tassin P, Zhuravel A P, Zhang L, Koschny T, Ustinov A V, Soukoulis C M and Anlage S M 2012 Switching nonlinearity in a superconductor-enhanced metamaterial *Appl. Phys. Lett.* **100** 121906
[26] Zhang C, Jin B, Han J, Kawayama I, Murakami H, Wu J, Kang L, Chen J, Wu P and Tonouchi M 2013 Terahertz nonlinear superconducting metamaterials *Appl. Phys. Lett.* **102** 081121
[27] Kang L *et al* 2011 Suppression of superconductivity in epitaxial NbN ultrathin films *J. Appl. Phys.* **109** 033908
[28] Glossner A, Zhang C, Kikuta S, Kawayama I, Murakami H, Muller P and Tonouchi M 2012 Cooper pair breakup in $YBa_2Cu_3O_7$−under strong terahertz fields arXiv:1205.1684v1
[29] Orenstein J, Bokor J, Budiarto E, Corson J, Mallozzi R, Bozovic I and Eckstein J N 1997 Nonlinear electrodynamics in cuprate superconductors *Physica* C **282–287** 252–5
[30] Grady N K *et al* 2013 Nonlinear high-temperature superconducting terahertz metamaterials *New J. Phys.* **15** 105016
[31] Vendik O G, Zubko S P and Nikol'skii M A 1999 Modeling and calculation of the capacitance of a planar capacitor containing a ferroelectric thin film *Tech. Phys.* **44** 349
[32] Rosa E B 1908 The self and mutual inductances of linear conductors *Bull. Natl Bur. Stand.* **4** 301–44
[33] Vendik O G, Vendik I B and Kaparkov D I 1998 Empirical model of the microwave properties of high-temperature superconductors *IEEE Trans. Microw. Theory Tech.* **46** 469–78
[34] Brorson S D, Buhleier R, Trofimov I E, White J O, Ludwig C, Balakirev F F, Habermeier H-U and Kuhl J 1996 Electrodynamics of high-temperature superconductors investigated with coherent terahertz pulse spectroscopy *J. Opt. Soc. Am.* B **13** 1979–93
[35] Melo A M, Angelo L G, Piazzetta Maria H O and da Silva M P A 2012 Cross-shaped terahertz metal mesh filters: historical review and results *Adv. Opt. Technol.* **2012** 530512
[36] Singh R, Chowdhury D R, Xiong J, Yang H, Azad A K, Taylor A J, Jia Q X and Chen H T 2013 Influence of film thickness in THz active metamaterial devices: a comparison between superconductor and metal split-ring resonators *Appl. Phys. Lett.* **103** 061117